Journal of Vacuum Science & Technology B

Atomic-resolution lithography with an on-chip scanning tunneling microscope

Afshin Alipour,[1] Emma L. Fowler,[1] S. O. Reza Moheimani,[1] James H. G. Owen,[2] and John N. Randall[2]
[1)]*Erik Jonsson School of Engineering and Computer Science, The University of Texas at Dallas, Richardson, Texas 75080, USA*
[2)]*Zyvex Labs LLC, 1301 N Plano Rd., Richardson, Texas 75081, USA*

(*Corresponding author: reza.moheimani@utdallas.edu)

(Dated: 5 April 2022)

In this work, atomic-resolution lithography with a Microelectromechanical-System (MEMS) based Scanning Tunneling Microscope (STM) is demonstrated for the first time. The microscope consists of a commercial Ultra-High-Vacuum (UHV) STM whose regular tip is replaced with a 1-Degree-of-Freedom (1-DOF) MEMS nanopositioner. This results in a hybrid STM system where XY-plane motions are provided by the piezotube of the original system, and Z-axis motion by the MEMS with higher bandwidth. Sharp tips made of Pt or W are added to the MEMS devices post fabrication. With this hybrid system, STM-based lithography is demonstrated on a H-passivated Si (100)-2×1 sample under UHV condition. Results prove the capability of the hybrid STM system for atomic-scale lithography. This capability, paired with the small footprint of the MEMS device, makes this approach a candidate for building a high-throughput parallel STM lithography platform by incorporating an array of 1-DOF MEMS devices that perform lithography in parallel.

I. INTRODUCTION

Shortly after the invention of the Scanning Tunneling Microscope (STM) in 1982[1], researchers discovered that under certain conditions of bias and tunnel current, it is possible to trigger chemical reactions on the sample surface by STM[2]. This discovery evolved into the STM-based lithography where the STM tip acts as a source of an electron beam to expose a monolayer resist[3]. In this process, the tunneling electrons provide the required energy to break the chemical bond between the resist and surface atoms, leaving active sites on the surface to subsequently react with other species.

Depending on the bias voltage, STM-based lithography can be carried out in two modes. At 6-10 V of bias, STM enters the Field Emission (FE) mode with an electron-beam spot size of about 5 nm. At this voltage range, the tunneling electrons possess enough energy to directly break the bond between the resist and surface atoms. On the other hand, running an STM at a voltage of 4 V or less keeps the STM in tunneling mode with an electron-beam spot size of about 0.6 nm. In this mode, known as Atomically Precise (AP) lithography mode, the tunneling electrons cumulatively increase the vibrational energy of the resist atom until its bond with the surface breaks[4]. Therefore, the yield of AP mode lithography is much lower than that of FE mode lithography[5]. However, the patterns made by STM in AP mode are of ultimate atomic resolution and precision due to the dual effects of tunnel current falling off exponentially with distance from the tip to surface and the highly non-linear dependence of H depassivation with current in the AP mode[4]. This capability sets STM apart from other lithography tools making it a superior alternative to Conventional Electron-Beam lithography (CEBL) whose precision is fundamentally limited to a few nanometers[4].

Despite this superiority, STM-based lithography has far less throughput than CEBL[5]. This downside is rooted in its single-tip scheme and slow scan speed, primarily caused by the bulkiness of its piezonanopositioner, which is usually a piezotube. In this regard, Microelectromechanical-System (MEMS) nanopositioners appear to be a promising substitution for the piezotubes. Due to their smaller mass, they can offer higher bandwidth, and their smaller footprint allows them to be used in an array configuration to increase the throughput of conventional STM[6].

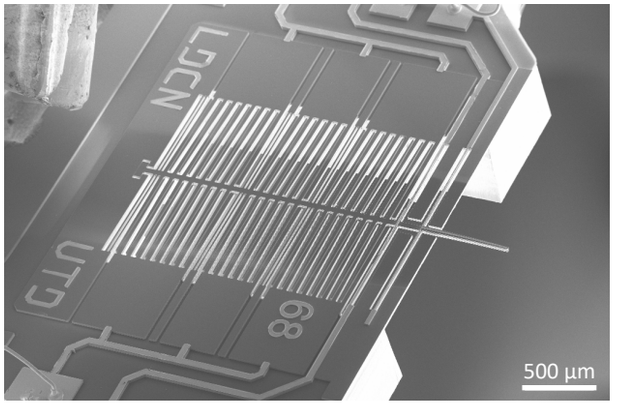

FIG. 1. SEM image of the 1-DOF MEMS STM Z-axis nanopositioner.

For accurate operation, the Z-axis bandwidth of the STM must be at least two, or preferably three orders of magnitude faster than its scan speed. We have developed 1-Degree-of-Freedom (1-DOF) MEMS nanopositioners to replace the Z axis of STM piezotubes that can operate an order of magnitude faster than the piezotube's Z-axis[7,8], therefore increasing the throughput of STM scanning or lithography by a factor of ten. The MEMS devices are designed to be mounted on the piezotube of a commercial Ultra-High-Vacuum (UHV) STM system to replace its regular tip. As a result, a hybrid STM system is achieved in which the XY-plane motions are delivered by the original piezotube, while the Z motion is provided by the MEMS device[9]. Figure 1 shows a Scanning-Electron-Microscope (SEM) image of a MEMS device used in the cur-

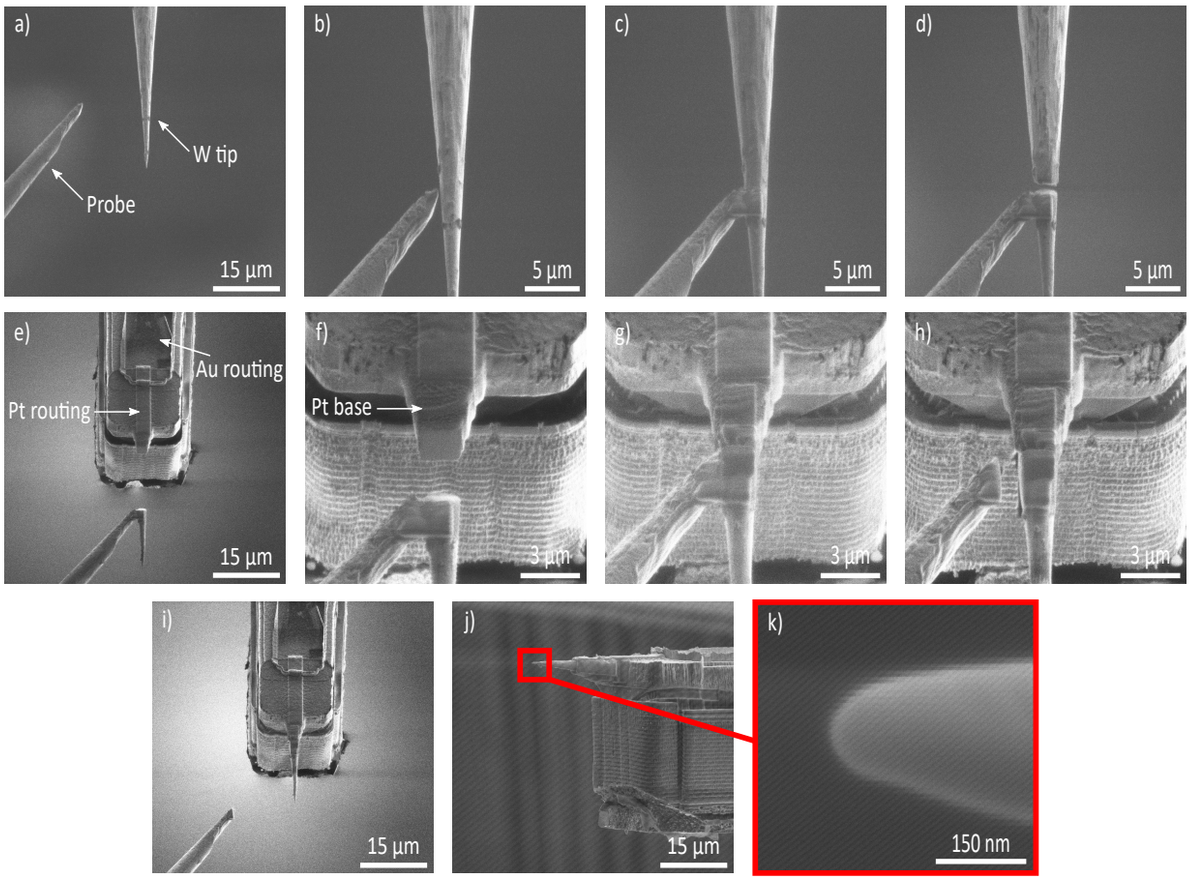

FIG. 2. Tip welding procedure: (a) the FIB probe is inserted, (b) the probe is moved close to the W tip, (c) Pt is deposited to join the probe and W tip, (d) the W tip is cut, (e) the probe is inserted with the MEMS device, (f) the probe is moved close to the MEMS device, (g) Pt is deposited to join the W tip, (h) the probe is etched, (i) the probe is removed, (j) the final assembled W tip, (k) the apex of the W tip.

rent work, which is based on the design presented in Ref. [7].

In this paper we demonstrate atomic-resolution STM-based lithography with the proposed hybrid system. Two types of tip material, Pt and W, are examined. Previously we discussed how to grow a Pt tip at the end of the MEMS' shuttle [7]. In Section II of the current manuscript we describe a procedure to add the apex of a pre-fabricated W tip to the MEMS device. The lithography experiments are then carried out based on the procedure laid out in Section III, and results are presented in Section IV for both tip types. Lastly, the article is concluded and future work is outlined in Section V.

II. TIP WELDING

Both Pt and W tips are used for atomic-resolution lithography. The Pt tips were simply made by depositing successively smaller rings of Pt on the MEMS device with a Focused-Ion-Beam (FIB) tool until a fine point was reached [7]. This Pt tip is then sharpened with the Field-Directed-Sputter-Sharpening (FDSS) process [10] and is ready to use. The remainder of this section will focus on an alternative post-fabrication technique, called tip welding, to place a W tip on the MEMS device.

To equip the MEMS device with a W tip, a traditional W STM tip was mounted vertically on a sample holder in the FIB, as shown by the SEM image in Fig. 2 a. After exercising eucentric height and setting the parameters for both electron and ion beams of the FIB, a probe is inserted until it is barely touching the W tip apex (Fig. 2 b). Induced by the ion beam, about 0.5 μm of Pt is deposited to join the W tip and the probe (Fig. 2 c).

The ion beam is then used to cut the W tip just above where the Pt was deposited on the probe (Fig. 2 d). The probe with the W tip apex on it is then slowly retracted from the remainder of the W tip that is on the sample holder. To affix the W tip apex to the MEMS device, the remainder of the W tip is replaced by the MEMS device in the FIB chamber (Fig. 2 e). If necessary, the base of the MEMS device where the W tip apex is to be affixed is etched with the ion beam so the base is smooth, or Pt is deposited if a taller base is needed. In addition, to ensure a full metal connection between the Pt base and Au routing used for the tunneling current signal, a 300-*nm*-thick Pt routing is deposited to join the two.

The probe is then re-inserted and brought approximately 5 μm from the MEMS base (Fig. 2 f). Using the lowest speed, the W tip is brought into contact with the MEMS base. Pt is

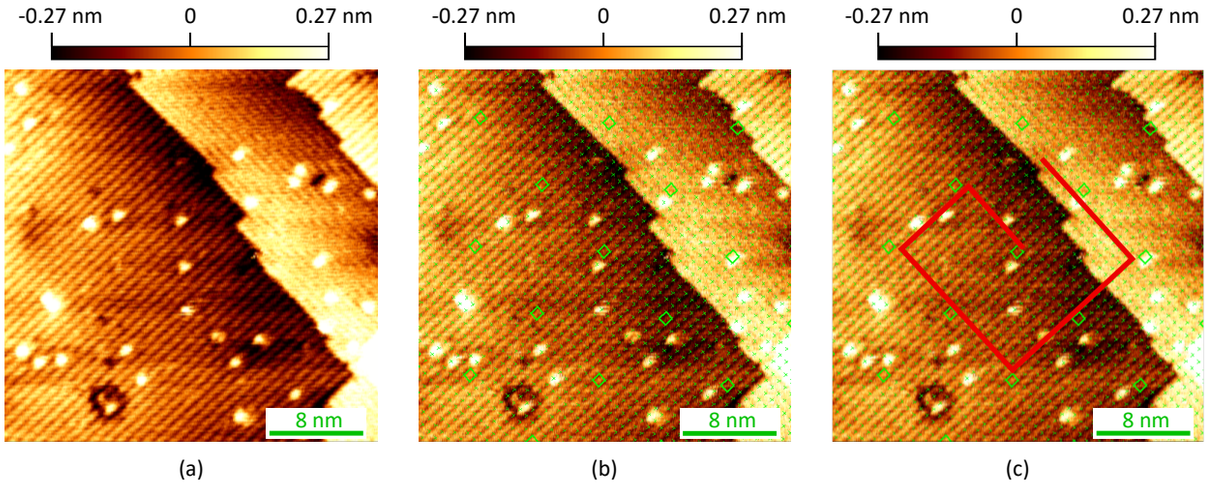

FIG. 3. STM-based lithography procedure: (a) the sample surface is first imaged, and (b) the lattice of the sample is detected and mapped. Afterwards (c), the trajectory along which the tip needs to move is defined with respect to the lattice.

then deposited to join the MEMS device and the W tip apex (Fig. 2 g). To remove the W tip from the probe, the probe is etched (Fig. 2 h). After fully separating the probe and the W tip, the probe is slowly retracted from the FIB chamber (Fig. 2 i) and more Pt is deposited around the W tip to reinforce the junction. Figures 2 j and k show the SEM images of the W tip assembled into the MEMS device. Similar to the previous Pt tips, the resulting tip is sharpened using the FDSS process.

The considerations mentioned in this section make the described tip welding technique highly repeatable. For instance, the thick Pt deposition joining the tip apex and probe prevents tip loss when transferring it to the MEMS device. However, it should be mentioned that even under skilled oversight, it can take up to three hours to equip each MEMS device with a W tip.

III. EXPERIMENT PROCEDURE

The proposed hybrid system is a Scienta Omicron UHV variable-temperature STM system in which the MEMS device replaces the piezotube's Z axis and the tip. Steps taken to integrate the MEMS device into the UHV system, and successful STM imaging of a H-passivated Si(100)-2×1 sample are described in our previous work [9], where we demonstrated imaging performance on a par with the original system. The sample consists of a single layer of H atoms adsorbed onto the Si surface to serve as a monolayer resist. In the current work, we utilize the hybrid system to pattern the resist layer by H depassivation.

In order to have better controllability over desorption of the H atoms along the sample's dimer rows, drift in the piezotube along the XY-plane is first identified and corrected by successive scanning of the surface with the hybrid system. After this correction, the surface is again scanned to obtain an STM image of the surface, which is shown in Fig. 3 a. Based on the STM scan, the lattice of the sample is detected and mapped onto the image (Fig. 3 b). Afterwards, the tip is moved along a predefined trajectory in the XY plane with respect to the lattice (solid line in Fig. 3 c), while the tunneling parameters are set to those required for STM-based lithography and the Z axis is kept in closed loop. Due to energy provided by the tunneling electrons, the H atoms along the trajectory will be desorbed, leaving a line of dangling bonds of Si atoms along the trajectory.

TABLE I. STM Parameters during lithography.

Experiment	Bias (V)	Setpoint (nA)	Dosage (mC/cm)	Writing speed (nm/s)
MEMS with Pt tip				
Figure 4 a	4	4	3	13.3
Figures 4 b and c	3.75	3	3	10
MEMS with W tip				
Figures 4 d and e	4	3	3	10
Figure 4 f	4	2	3	6.6

IV. RESULTS

Based on the lithography procedure laid out in the previous section, single-loop spiral patterns are made in the H layer of the sample. For the sake of comparison, the lithography parameters are chosen to be similar to those commonly used in conventional STMs to produce single-dimer-row resolution patterns in AP mode. For a bias of $4\,V$ and a setpoint of $2\,nA$, writing speeds ranging from $2\,nm/s$ to $20\,nm/s$ have been reported in the literature[11]. The parameters used in our experiments are reported in Table I

In the first set of lithography patterns presented in Figs. 4 a-c, a MEMS device with a Pt tip is employed in the hybrid system. As evident from the results, the proposed system was

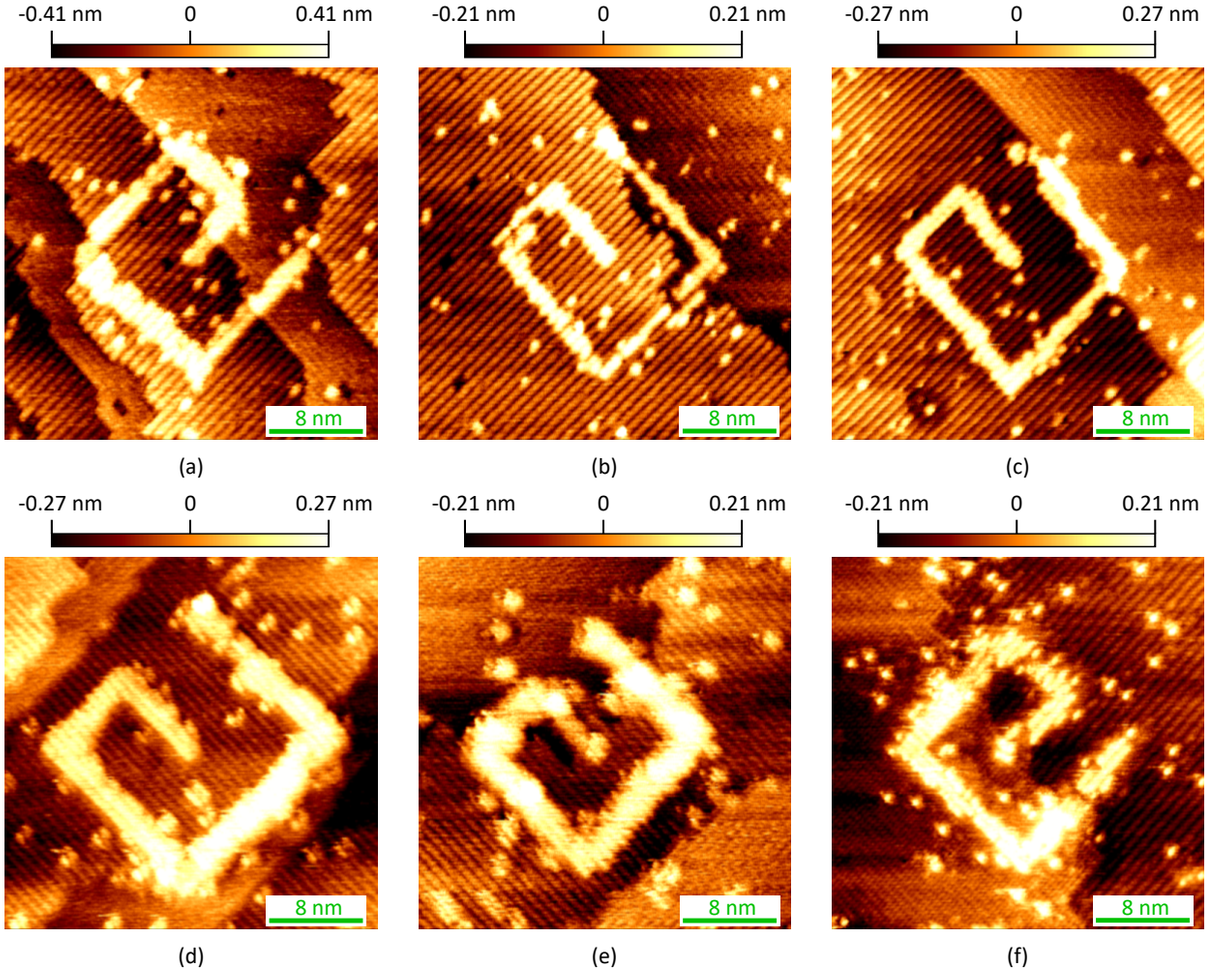

FIG. 4. Patterns made in the resist layer of the sample with the hybrid STM system incorporating a MEMS device with a (a)-(c) Pt tip and (d)-(f) W tip. The bias and current setpoint used for the STM images of (a)-(c) range from -1.25 V to -1.5 V and from 0.1 nA to 0.2 nA, respectively. Images of (d)-(f) are obtained under bias of -1 V and current setpoint ranging from 0.8 nA to 1 nA. Tip speed during all the scans was 312.5 nm/s.

able to produce lithography patterns with atomic-resolution. Regarding resolution, the pattern in Fig. 4 a is of two- to three-wide dimer-row resolution. By lowering the bias and setpoint during the lithography, finer patterns could be achieved, even down to single-dimer-row resolution as in Fig. 4 b. In terms of writing speed, which corresponds to the lithography throughput, speeds of 10 nm/s and 13.3 nm/s are demonstrated with our hybrid system. These writing speeds are within the range expected from previous attempts with conventional STMs to achieve single-dimer-row patterns [11].

In the second set of experiments, the MEMS device is equipped with a W tip. Figures 4 d-f present three lithography patterns obtained with this MEMS device. The patterns of Figs. 4 d and e are of a slightly lower resolution than those obtained with a Pt tip, which is due to the double-tip situation for this particular W tip, indicating the importance of tip shape in lithography.

V. CONCLUSION

The throughput of conventional STM-based lithography is inherently limited. Motivated by addressing this issue, we designed and fabricated a 1-DOF MEMS nanopositioner to replace the Z-axis of STM piezotube used in conventional STMs. After integrating the MEMS nanopositioners with Pt and W tips into a commercial UHV STM, we demonstrated atomic-resolution lithography with our proposed hybrid STM on a par with conventional STMs.

The high bandwidth and small footprint of this MEMS device makes it possible to use an array of such MEMS devices in parallel to drastically increase the throughput of conventional STM lithography, which is a goal of our future work. To achieve this, we will develop a custom-made 2-DOF piezo-nanopositioner for XY-motions and integrate it into a UHV system. This will allow the scanner head, unlike the commercial UHV STM system, to have a sufficient number of signal pins for a 1-DOF array of MEMS STM nanopositioners.

VI. ACKNOWLEDGMENTS

This material is based upon work supported by the U.S. Department of Energy's Office of Energy Efficiency and Renewable Energy (EERE) under the Advanced Manufacturing Office Award No. DEEE0008322. The authors wish to thank Zyvex Labs members, Robin Santini for his assistance in setting up the experimental testbeds, and Ehud Fuchs for fruitful discussions. They also wish to thank Abhas Mehta for his invaluable assistance in the tip welding process.

VII. AUTHOR DECLARATIONS

A. Conflict of interest

The authors have no conflicts to disclose.

VIII. DATA AVAILABILITY

The data that supports the findings of this study are available within the article.

[1]G. Binnig, H. Rohrer, C. Gerber, and E. Weibel, "Tunneling through a controllable vacuum gap," Applied Physics Letters **40**, 178–180 (1982), https://doi.org/10.1063/1.92999.

[2]M. Ringger, H. R. Hidber, R. Schlögl, P. Oelhafen, and H. Güntherodt, "Nanometer lithography with the scanning tunneling microscope," Applied Physics Letters **46**, 832–834 (1985), https://doi.org/10.1063/1.95900.

[3]J. W. Lyding, T. Shen, J. S. Hubacek, J. R. Tucker, and G. C. Abeln, "Nanoscale patterning and oxidation of h-passivated si(100)-21 surfaces with an ultrahigh vacuum scanning tunneling microscope," Applied Physics Letters **64**, 2010–2012 (1994), https://doi.org/10.1063/1.111722.

[4]J. N. Randall, J. H. G. Owen, J. Lake, and E. Fuchs, "Next generation of extreme-resolution electron beam lithography," Journal of Vacuum Science & Technology B **37**, 061605 (2019), https://doi.org/10.1116/1.5119392.

[5]J. N. Randall, J. W. Lyding, S. Schmucker, J. R. Von Ehr, J. Ballard, R. Saini, H. Xu, and Y. Ding, "Atomic precision lithography on si," Journal of Vacuum Science & Technology B: Microelectronics and Nanometer Structures Processing, Measurement, and Phenomena **27**, 2764–2768 (2009), https://avs.scitation.org/doi/pdf/10.1116/1.3237096.

[6]M. Bulut Coskun, M. Baan, A. Alipour, and S. O. Reza Moheimani, "Design, fabrication, and characterization of a piezoelectric afm cantilever array," in *2019 IEEE Conference on Control Technology and Applications (CCTA)* (2019) pp. 227–232.

[7]A. Alipour, M. B. Coskun, and S. O. R. Moheimani, "A high bandwidth microelectromechanical system-based nanopositioner for scanning tunneling microscopy," Review of Scientific Instruments **90**, 073706 (2019), https://doi.org/10.1063/1.5109900.

[8]A. Alipour, M. B. Coskun, and S. O. R. Moheimani, "A mems nanopositioner with integrated tip for scanning tunneling microscopy," Journal of Microelectromechanical Systems **30**, 271–280 (2021).

[9]A. Alipour, S. O. R. Moheimani, J. H. G. Owen, E. Fuchs, and J. N. Randall, "Atomic precision imaging with an on-chip scanning tunneling microscope integrated into a commercial ultrahigh vacuum stm system," Journal of Vacuum Science & Technology B **39**, 040603 (2021), https://doi.org/10.1116/6.0001107.

[10]S. W. Schmucker, N. Kumar, J. R. Abelson, S. R. Daly, G. S. Girolami, M. R. Bischof, D. L. Jaeger, R. F. Reidy, B. P. Gorman, J. Alexander, *et al.*, "Field-directed sputter sharpening for tailored probe materials and atomic-scale lithography," Nature communications **3**, 1–8 (2012).

[11]S. Chen, H. Xu, K. Goh, L. Liu, and J. Randall, "Patterning of sub-1 nm dangling-bond lines with atomic precision alignment on h: Si (100) surface at room temperature," Nanotechnology **23**, 275301 (2012).

IX. FIGURE CAPTIONS

1. SEM image of the 1-DOF MEMS STM Z-axis nanopositioner.

2. Tip welding procedure: (a) the FIB probe is inserted, (b) the probe is moved close to the W tip, (c) Pt is deposited to join the probe and W tip, (d) the W tip is cut, (e) the probe is inserted with the MEMS device, (f) the probe is moved close to the MEMS device, (g) Pt is deposited to join the W tip, (h) the probe is etched, (i) the probe is removed, (j) the final assembled W tip, (k) the apex of the W tip.

3. STM-based lithography procedure: (a) the sample surface is first imaged, and (b) the lattice of the sample is detected and mapped. Afterwards (c), the trajectory along which the tip needs to move is defined with respect to the lattice.

4. Patterns made in the resist layer of the sample with the hybrid STM system incorporating a MEMS device with a (a)-(c) Pt tip and (d)-(f) W tip. The bias and current setpoint used for the STM images of (a)-(c) range from -1.25 V to -1.5 V and from 0.1 nA to 0.2 nA, respectively. Images of (d)-(f) are obtained under bias of -1 V and current setpoint ranging from 0.8 nA to 1 nA. Tip speed during all the scans was 312.5 nm/s.

Journal of Vacuum Science Technology B

PLEASE CITE THIS ARTICLE AS DOI: 10.1116/6.0001826

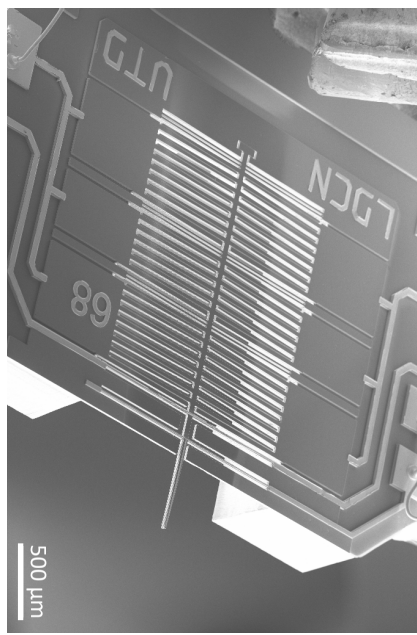

Journal of Vacuum Science Technology B

Journal of Vacuum Science Technology B

PLEASE CITE THIS ARTICLE AS DOI: 10.1116/6.0001826

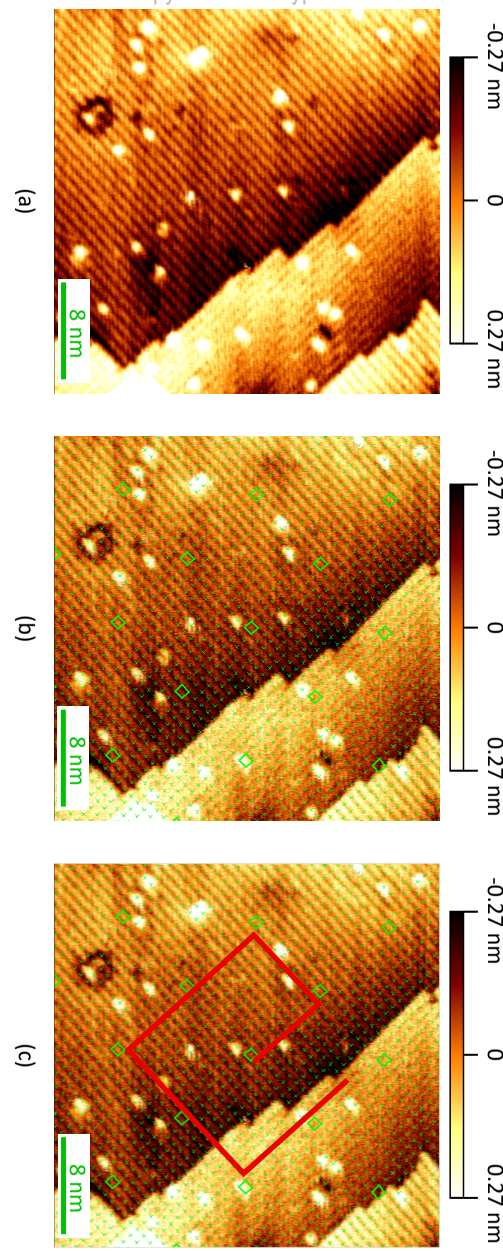

Journal of Vacuum Science Technology B